Can cirrus clouds produce glories?

Kenneth Sassen, W. Patrick Arnott, Jennifer M. Barnett, and Steve Aulenbach

A vague glory display was photographed over central Utah from an airplane beginning its descent through a cirrus cloud layer with an estimated cloud top temperature of −45 and −55 °C. Photographic analysis reveals a single reddish-brown ring of 2.5–3.0° radius around the antisolar point, although a second ring appeared visually to have been present over the brief observation period. Mie and approximate nonspherical theory scattering simulations predict a population of particles with modal diameters between 9 and 15 μm. Although it is concluded that multiple-ringed glories can be accounted for only through the backscattering of light from particles that are strictly spherical in shape, the poor glory colorization in this case could imply the presence of slightly aspherical ice particles. The location of this display over mountainous terrain suggests that it was generated by an orographic wave cloud, which we speculate produced numerous frozen cloud droplets that only gradually took on crystalline characteristics during growth.

OCIS codes: 010.1290, 010.1310.

1. Introduction

Because they produce optical phenomena like haloes and arcs, high-altitude cirrus clouds have long been known to consist of nonspherical ice crystals that show a variety of hexagonal particle habits and orientations.[1] In contrast, water droplet clouds are associated with optical displays such as the backscatter glory and cloudbow, which Mie theory demonstrates are produced by spherical scatterers.[2] However, the case for the forward-scattering corona has been shown to be ambiguous, for diffraction effects in fairly monodispersed assemblies of cloud droplets,[3] ice crystals,[4,5] and even tree pollen[6] are all capable of generating coronas. Strong laser light backscatter depolarization[4] and recent *in situ* particle sampling have verified that corona-producing cirrus clouds contain particles that are far from spherical in nature.[5]

On the other hand, recent *in situ* studies have suggested that small, near-spherical ice particles (which we refer to as aspherical) can occur near the tops or along the margins of some ice clouds. The photomicrographs of Fig. 1, for example, show ice crystals collected by impaction with a balloonborne Formvar replicator device[7] from a cirrus wave cloud at temperatures between −40 and −50 °C. Some of these particles have grown into identifiable hexagonal columns or appear to be faceted uniaxial polyhedral crystals, but others clearly resemble spheres. But the question is whether they display sufficient spherical symmetry to create the glory. It is well known from Mie theory[2,8] that the glory results from the interference of light rays backscattered from two different mechanisms: internally reflected and circumferential (i.e., surface wave) ray paths, the latter of which is unique to spheres.

In this paper, we present unique photographic evidence for the possible occurrence of a cirrus cloud glory (or other unknown phenomenon), provide an assessment of the likelihood for the existence of spherical ice particles, briefly examine alternative hypotheses for the existence of this retroreflection display, and then consider the amount of nonsphericity needed to inhibit glory formation in aspherical particles. Our conclusions as to the nature of the optical display are given in Section 5.

2. Photographic Evidence

On 20 January 1995, a retroreflection phenomenon was photographed over central Utah from an airplane passing through the 10.7-km above mean sea level as it began its descent into Salt Lake City International Airport. Photographs were taken at around 2357 UTC using a 35-mm camera with a 24-mm wide-angle lens. The cirrus cloud layer was geographically widespread and optically thin enough

K. Sassen and J. M. Barnett are with the Department of Meteorology, University of Utah, Salt Lake City, Utah 84112. W. P. Arnott is with the Desert Research Institute, Atmospheric Sciences Center, Reno, Nevada 89506. S. Aulenbach is with the National Center for Atmospheric Research, MMM, Boulder, Colorado 80307.

Received 23 June 1997; revised manuscript received 31 October 1997.

0003-6935/98/091427-07$15.00/0

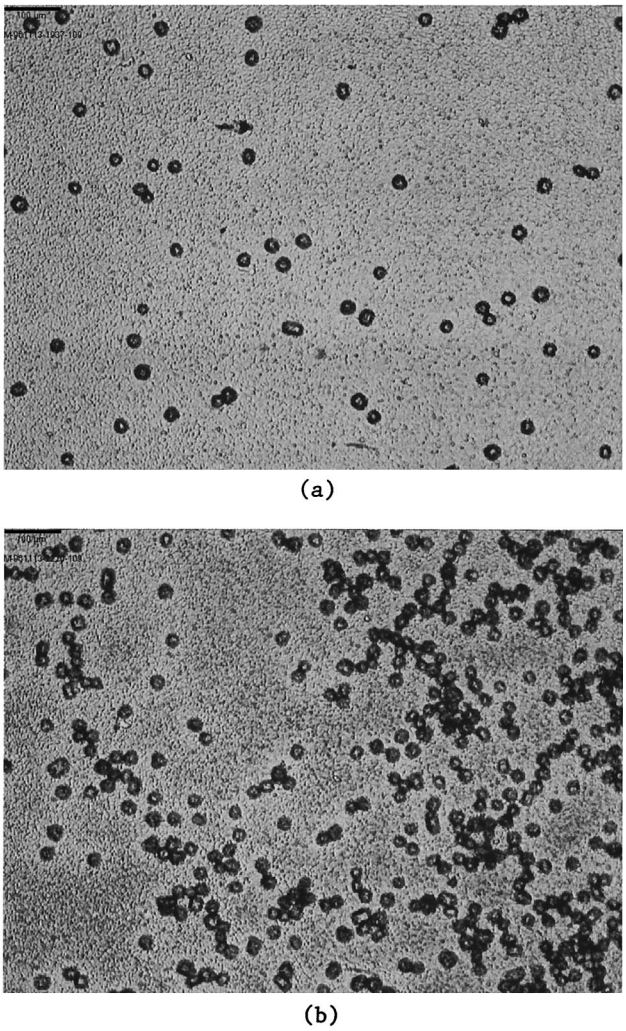

Fig. 1. Photomicrographs of newly formed ice crystals sampled from a cirrus wave cloud over Boulder, Colo., on 13 November 1996, collected at (a) −40.0 °C and 9.35 km, (b) −48.6 °C and 10.13 km. For scale, note that the bars at top left are 100 μm in length.

to view the snow-covered Wasatch Mountain Plateau beneath the cloud when one was looking down through the aircraft window. The apparent glory was easily visible as a reddish-brown ring surrounding the shadow of the aircraft, ahead of that of a short contrail. Analysis of the three photographs collected (e.g., Fig. 2) shows only a single ring surrounding a central bright spot, although a vague second ring appeared visually to have been present over the brief (~3-min) observation period. The angular radius of the ring center varied from 2.5° to 3.0° during several measurements of the enlarged images.

3. Alternative Explanations

As a result of its association with the contrail shadow shown in Fig. 2, there is no doubt that the glorylike display is centered at the antisolar point. The 2.5°–3.0° ring radius is consistent with stratus cloud red glory rings[9] but is inconsistent with any known hexagonal (or other habit) ice-crystal halolike display. (Moreover, this display is notable because of the presence of a dark ring, and not a bright ring, at the potential angle of minimum deviation.) The only other known antisolar point display is the rare antisolar spot, or anthelion,[10] which is usually (if not solely) seen in association with the subparhelic circle. We provide an example of this seldomly photographed display in Fig. 3 for comparison with Fig. 2. This image of the antisolar spot along with a segment of the subparhelic circle was obtained over western New York at 11.3-km altitude while the plane was flying just above the extensive cirrus shield created by the outflow of (former) hurricane Josephine on the afternoon of 8 October 1996. The dissimilarities between the presumed ray-interference cirrus glory and the anthelion–subparhelic circle (created by internally reflected rays from horizontally oriented crystals) are obvious.

The coincident Salt Lake City radiosonde data indicate a likely cirrus cloud top temperature in the −45 to −55 °C range, thus excluding the possibility of such highly supercooled cloud droplets existing near cloud top long enough to generate a glory without freezing homogeneously into ice particles. The brief appearance of this display and its location over mountainous terrain suggest that the cloud-generating mechanism was a mountain wave located at approximately the cirrus cloud top position: the sharpness of the contrail shadow outline and lack of any visible lower cloud layers gave a strong impression that the display was generated close to the cloud top, as has also been deduced to occur in water clouds because of the effects of multiple scattering further into the cloud.[9] It is possible that lower-level supercooled orographic water clouds could have been present below the cirrus, but these would not have had an impact because of the great optical depth produced when one was looking nearly horizontally into the cirrus cloud layer (i.e., because the observations were made at ~5 p.m. local time near midwinter, the Sun was close to setting). Also note that the angular size of the shadow of the contrail immediately behind the aircraft implies that the cloud top was not far below the aircraft when the photographs were taken.[11]

4. Theoretical Considerations

A. Mie Theory Results

The unique backscattering response of small (relative to visible wavelengths) cloud droplets to create the glory was rarely appreciated, and mostly by early mountain climbers, until the advent of frequent air transportation. The rigorous dielectric sphere scattering theory of Mie can be used to simulate the glory, although an appreciation of the key geometric properties of glory scattering was first expressed by van de Hulst.[8] The incident ray in Fig. 4(a) couples to the sphere as a surface wave, is critically refracted into the sphere, reflects off of the sphere, is again critically refracted to the surface, and after a short path as a surface wave, the (glory) ray is directed backward. A curved wave front is formed by the exiting rays to the right and the left of the glory ray.

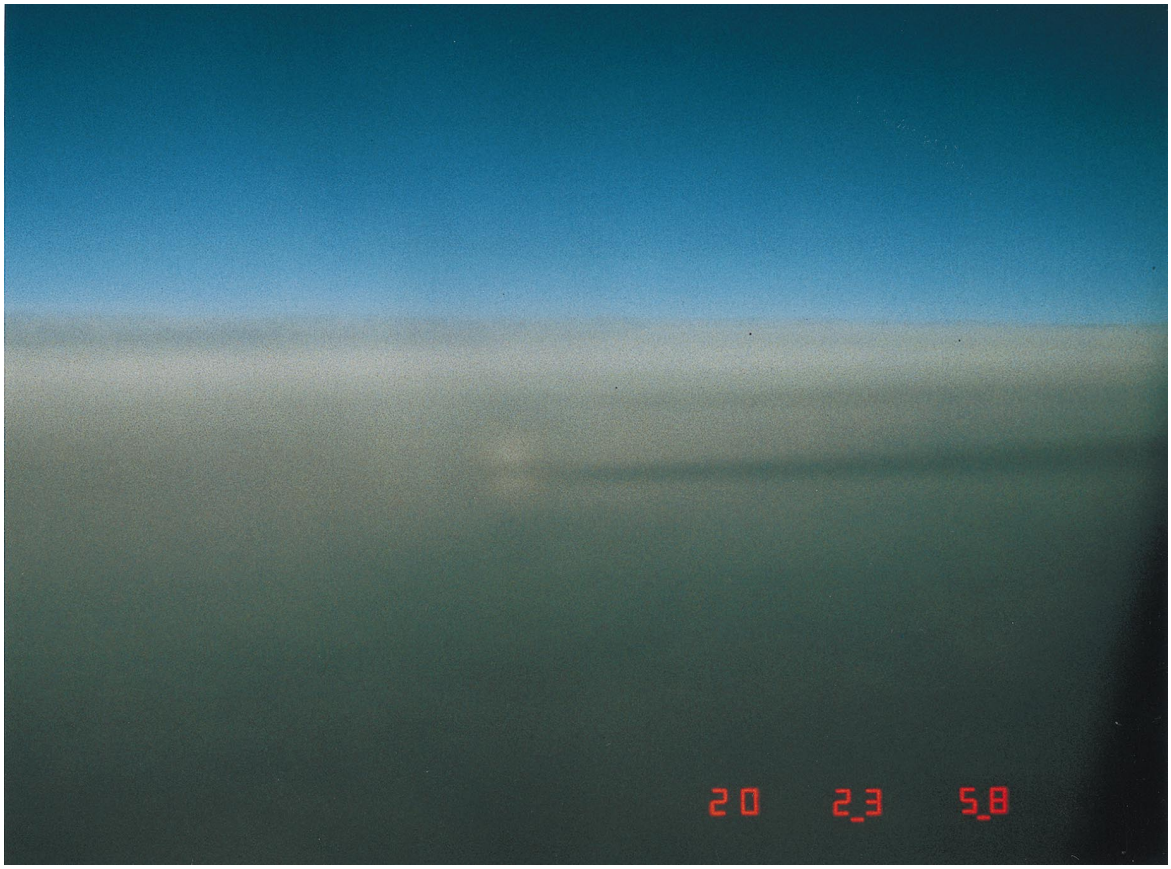

Fig. 2. Wide-angle aerial photograph of a vague glory display taken just before the aircraft started its descent through a cirrus cloud layer at 2358 UTC on 20 January 1995.

Rotating this curved wave front through an angle π (as dictated by spherical symmetry) reveals that the wave-front shape associated with the glory is a toroid, as illustrated in Fig. 4(b). Propagation of this wave front to the far field gives rise to strong axial focusing because rays from the ring around the flat part of the wave front are all headed in the same direction. In fact, an infinite number of such rays exist on this ring. As soon as the observation point moves off of the exact backward direction, only two rays now contribute to the scattering, one each from the left-hand and the right-hand sides of the toroidal wave front. It is the interference of these rays that produces the colorful rings associated with the glory.

Our approach here is not a rigorous one: we use Mie theory to understand the relation between the droplet size and the radius of the glory rings in order to help interpret the photographic measurements by means of passive remote sensing. Before the predictions are given, however, it is important to note that, because of the strongly size-dependent nature of the interference phenomenon, it is essential to use a distribution of droplet sizes to average out the effects of strong scattering resonances. Because cloud particle-size distributions in nature are highly variable, we use as an approximation the zeroth-order logarithmic distribution[12] given below, which has the property of the modal radius r_m remaining constant as the standard deviation σ_0 of the distribution is changed. The distribution expressed in terms of the probability P of particles with radius r is

$$P(r) = \frac{\exp\left[-\dfrac{(\log r - \log r_m)^2}{2\sigma_0{}^2}\right]}{(2\pi)^{1/2}\sigma_0 r_m \exp(\sigma_0{}^2/2)}. \quad (1)$$

To keep the distributions narrow enough to avoid washing out the glory effect in clouds and still limit interference fluctuations, after experimentation we have varied σ_0 along with r_m in such a way as to retain a peak distribution probability of $P(r) = 1.0$ at r_m. The resultant log-normal size distributions are illustrated in Fig. 5 for three r_m. Although these rather narrow size distributions may not necessarily resemble those found in glory-producing clouds, at least with the use of the $P(r_m) = 1.0$ approach we do not have to arbitrarily specify σ_0.

Thus we now show in Fig. 6 the results of Mie theory predictions of the glory peaks for red (0.63-μm) light at the three indicated r_m for ice spheres (with refractive index $n = 1.31$). The red glory bands are depicted as the series of phase-function peaks to the left of the main backscatter maximum at $\theta = 180°$, which tend to decline rapidly in intensity with decreasing angle (i.e., with increasing glory

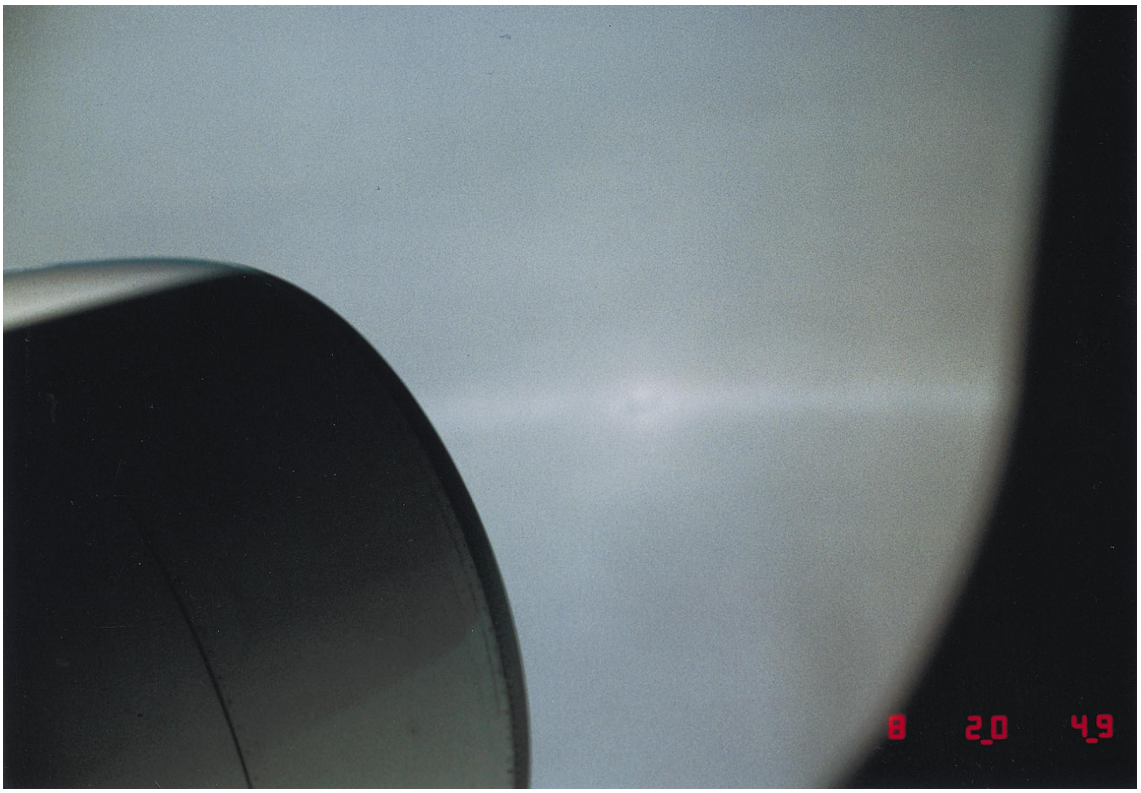

Fig. 3. Aerial photograph taken with a 55-m lens of the rare anthelion with a segment of the subparhelic circle, taken at 2049 UTC on 8 October 1996 above the cirrus cloud shield produced by hurricane Josephine.

band order). Although this analysis is hardly exhaustive, it shows that the visibility of glories depends on the modal radius. Spheres that are too small spread out weak rings over large angles, and those that are larger have rings that are packed closely together with intensities that pale in comparison with the true backscatter peak. Obviously the effects of mean particle size and the width of the distribution on the colorization and visibility of the glory will also be significant, but these aspects are beyond the scope of the current work.

The effects of varying the ice-sphere radius on the glory ring positions (assuming that the red rings correspond to the 0.63-μm wavelength phase-function peaks) are shown in Fig. 7 for the first three orders. These results also show the narrowing between the bands as the sphere radius increases. Although it is uncertain how accurate the derivation of particle size would be with these results and glory angle measurements because of the final colorization properties when all wavelengths are considered together, in our

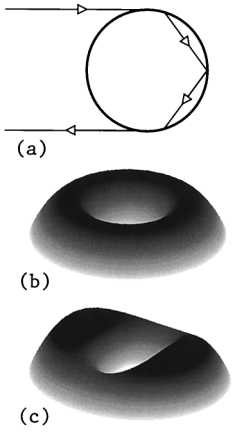

Fig. 4. Schematic representation of (a) the ray paths, (b) the toroidal wave front of backscattered light responsible for glory formation. A distorted toroidal wave front for slightly nonspherical particles is shown in (c).

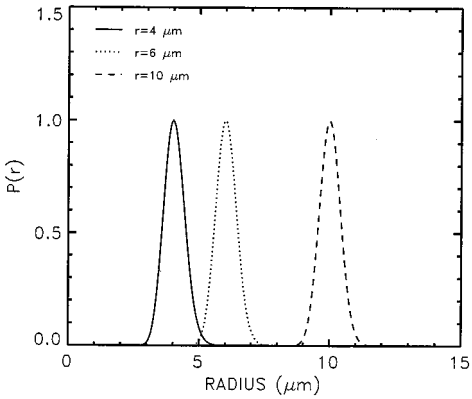

Fig. 5. Examples of the shapes of zeroth-order logarithmic particle-size distributions created to simulate polydisperse clouds.

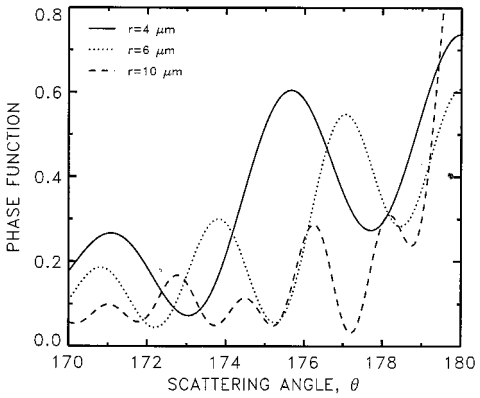

Fig. 6. Mie theory predictions of the phase functions in the backscattering region for populations of spheres with the indicated modal radii, showing the effects of particle size on the glory ring maxima.

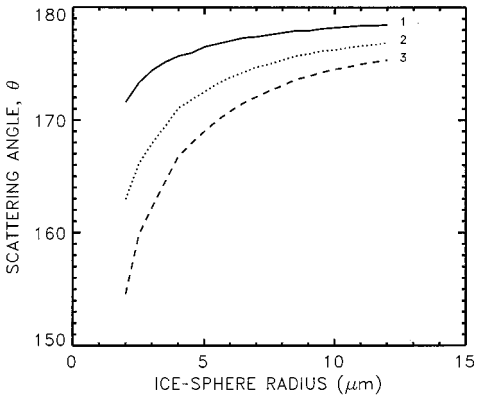

Fig. 7. Results from Mie theory of the angular position of the first- through third-order red-colored glory rings as a function of the modal ice-sphere radii between 2 and 12 μm.

case the first-order radii of 2.5°–3.0° (θ = 177°–177.5°) implies the presence of 12–15-μm mean-diameter ice spheres.

B. Approximate Theory Results

Because there is evidence for near-spherical ice particles under apparently similar conditions as those surmised here, but no unambiguous evidence for true ice spheres in tropospheric cirrus clouds, it is important to attempt to assess the limits in particle nonsphericity that can still permit the formation of a glory. In our investigation of the display shown in Fig. 2, it is clear that this would be a poor example of a glory—only a vaguely colored single ring is apparent—despite having favorable angles for reported glories.[9] This could signify a certain amount of ice-particle nonsphericity.

The potentially strong influence of nonsphericity on the glory was recognized by van de Hulst in his 1947 paper[8]:

> "It is obvious that the interference of rays which are refracted by opposite sides of a water drop will be much more sensitive to slight deformations of the droplets than are the rainbows in which only adjacent rays interfere, or the common coronas in which non-refracted rays interfere."

Fahlen and Bryant[13] observed this sensitivity in their surface wave observations from rather large pendant droplets illuminated by a He–Ne laser. They found that as the suspended droplet evaporated and became more spherical, surface waves became more uniformly bright. As we begin the difficult task of attempting to quantify the influence of nonsphericity on the glory, we define an oblate spheroidal particle characterized by an oblateness parameter Γ, given as $\Gamma = D^2/H^2 - 1$, where D is the equatorial diameter and H is the semiminor axis length of the ellipse that generates the oblate spheroid on rotation through an angle π. We do not imply that ice crystals can be treated as spheroids, but instead we attempt to make a connection with previous efforts at quantifying the effects of nonsphericity on the glory for which the particle shape was oblate spheroidal. The second useful nondimensional parameter that characterizes this problem is of course the size parameter x, defined as $x = \pi D/\lambda$, where λ is the wavelength of light.

The heart of the problem we are confronted with is how much the toroidal wave-front shape shown in Fig. 4(b) for spheres can be deformed and yet still allow the observation of more or less the same glory. We first shift the discussion to wave-front distortion and then link back to the particle shape that might give such distortion. We start in the realm of geometric optics, in which the size parameter $x \to \infty$, and move finally to more realistic finite wavelengths.

By analogy, the glory is perhaps simpler to understand in the underwater world in which air bubbles play the scattering role. Snell's law and the Fresnel coefficients are sufficient to describe the wave field near the bubble.[14] Backward-directed glory rays are associated with ray paths that have three or more chords inside the bubble. A toroidal wave front, as shown in Fig. 4(b), is pertinent to this problem as well.[14,15] To observe glory scattering by air bubbles in the laboratory, a water-filled scattering chamber was used along with a horizontal laser beam. Vertically rising air bubbles were produced that in some cases were sufficiently small ($D < 300$ μm), such that hydrodynamic forces were insufficient to distort their shape appreciably from spherical. These small bubbles exhibit glory scattering, as expected from Mie theory, and a physical optics approximation was developed that agreed well with Mie theory.[15] Later, larger bubbles (300 μm $< D <$ 700 μm) were produced that gave backscattering quite different from glory scattering.[16] In this size range the bubble shape is oblate spheroidal, with oblateness Γ increasing with D. The axial point caustic (literally, the burning spot, like the focal point of a magnifying glass) of glory scattering for spherical bubbles is said to unfold to an astroid caustic for oblate spheroidal bubbles. (The astroid figure can be illustrated by four identical coins that are placed side by side so

that a square encompasses all four coins: the curve formed along the inside boundary of the coins is an astroid.)

The distorted wave-front shape is shown in Fig. 4(c) for oblate bubbles illuminated with a laser beam parallel to the equatorial plane. Whereas an infinite number of rays are exactly backscattered in the glory of spherical bubbles, only four rays are so scattered for oblate bubbles.[16] The inside of the astroid caustic is a four-ray interference region, although beyond the caustic boundary, two rays interfere and produce rings rather similar to the glory of spherical bubbles. We might even go so far as to say that the main influence of nonsphericity in backscattering by oblate bubbles is confined to the inside of the astroid caustic. Let us call this the geometric boundary and understand it to be the angular-scattering boundary beyond which the effects of nonspherical scattering are negligible. Various studies have provided measured and simulated examples of rather striking features of the unfolded glory of oblate spheroidal bubbles.[16,17]

The angle of the geometric boundary relative to the backscattering direction can be estimated with the method outlined in Ref. 20. Here we use γ as the backscattering angle, where $\theta = \pi - \gamma$. For $\tan(\gamma) \approx \gamma$, the angle of the geometric boundary can be obtained as[17]

$$\gamma = 2\delta/b, \tag{2}$$

where $b \approx D/2$ is the radius of the focal circle that the toroidal wave front appears to emanate from and δ is the difference in the propagation phase delay of glory rays in the equatorial and the elliptical planes of the spheroid. Approximating the path of a glory ray as a surface wave that couples to the spheroid at a point of tangency and exits after propagating half the perimeter of the equatorial or elliptical planes and keeping terms to first order in Γ gives

$$\gamma = n\pi\Gamma/2. \tag{3}$$

We can now make an estimate for the upper bound of permissible oblateness. Because the outer ring of the apparent glory of Fig. 2 was measured at $\sim 3.0°$, the geometric boundary γ should lie within the angle of this ring. Thus $\gamma = 3.0°$ yields $\Gamma \approx 0.026$ or $D/H \approx 1.013$. We have arrived at a result that is consistent with van de Hulst's comment quoted above: "The glory does not tolerate much nonsphericity."

A perhaps surprising feature of Eq. (3) is that both λ and D do not appear explicitly. We have implicitly included them, though, through use of the observed color ring angle. Larger D would naturally have produced a smaller angle for the observed ring. An estimate of the relation of particle size to ring angle can be obtained by consideration of the first minimum in the backscattering pattern of an acoustic bubble.[17] This relationship is

$$\pi - \theta = 2.405\lambda/(\pi D). \tag{4}$$

Combining Eqs. (3) and (4) now yields

$$\Gamma = 4.81\lambda/(n\pi^2 D) \tag{5}$$

for the maximum oblateness the glory can tolerate. The interpretation of Eq. (5) is that one should expect to observe a glory if the oblateness is less than the quantity given by this relation.

This nonsphericity estimation was derived for oblate spheroidal bubbles under a specific orientation that emphasized nonsphericity. However, bubbles illuminated by laser light incident along the axis of rotational symmetry of the spheroid may still give a glory. It is reasonable to assume that backscattering by a cloud of randomly oriented, substantially oblate spheroidal bubbles might still produce a weak glory, even though the specific orientation of the bubble with symmetry axis perpendicular to the illumination would not produce a glory. Ice particles small enough to have produced the observed less-than-spectacular glory would certainly be randomly oriented, so this could be expected to loosen the rather stringent criteria suggested by Eq. (5). Importantly, this conclusion is supported by the phase functions derived from randomly oriented spherically deformed Chebyshev particles by use of the T-matrix approach, which preserves glory maxima for slight, but not minuscule deformations,[18] and by the results of Asano and Sato,[19] which a show weak glorylike maximum near $\theta = \pi$ for the case of randomly oriented oblate spheroids with $x = 15$ and an axis ratio of 2. We believe that further physical insight into the question of the nonspherical particle glory awaits suitable computations based on Maxwell's equations, a daunting task.

Finally, applying Eq. (4) to the estimation of the equivalent particle size producing our reddish ring at 2.5° to 3.0°, using $\lambda = 0.63$ μm as above, we obtain particle diameters of 9.2–11.1 μm. This compares with the 12–15-μm sizes found from the simple Mie theory analysis described above.

5. Conclusions

Because of fundamental spherical particle scattering principles, the multiple-ringed glory phenomenon, like the cloudbow, must remain within the exclusive domain of water droplet clouds until strong evidence proves otherwise. Current understanding of the physics of ice-crystal growth under tropospheric conditions indicates that spherical ice particles should not exist, at least not long after the nucleation of an initially spherical haze or cloud droplet. Only at unlikely frigid temperatures (for our atmosphere) should ice grow in amorphous (and presumably spherical) shapes.[20] Nonetheless, this issue has relevance to climate research because the shapes and sizes of cirrus cloud particles are crucial to understanding their radiative impact. Ironically, although considerable effort has gone into developing the means to treat the scattering behavior of nonspherical particle shapes, in contrast to the relative ease of Mie theory, is it possible that some cirrus

cloud contents could be adequately treated in terms of ice spheres?

We conclude that the only satisfactory explanation for the apparent cirrus cloud glory described here is an orographically generated cloud composed of aspherical (also known as quasi-spherical or near-spherical) ice particles. Although it seems unlikely to show this rigorously with current scattering theories, the necessary condition for the generation of a vague glory may be newly formed ice crystals that retain a measure of the initial spherical shape of the frozen droplet, at least in certain planes through the droplet's center. Ice particles that apparently meet this criterion are not unknown from earlier studies in ice fogs[21] and laboratory cloud chambers,[22,23] as well as the new photomicrographic evidence presented here in Fig. 1. It may be that these kinds of aspherical ice particles are not uncommon to cirrus wave clouds, in which their formation is favored by strong updrafts and the formation of high concentrations of ice crystals from homogeneously frozen cloud droplets or haze particles: their shapes may reflect the severe competition effects for the available moisture on ice-particle growth. Alternatively, perhaps rapidly sublimating ice crystals in the wave downdraft (as suggested by a reviewer) could also create suitably aspherical particles. Our analyses of the apparent glory photograph by using Mie and approximate theory approaches yields particle diameters ranging from 9 to 15 μm.

It is our hope that this study will stimulate further theoretical research and a great deal more casual observations from aircraft of the antisolar point to search for better explanations and additional examples of this phenomenon. In searching for cirrus cloud glories, a polarizing filter would be useful in identifying true glories because of their strong negative polarization.[24]

This research has been supported by U.S. National Science Foundation grant ATM-9528287. W. P. Arnott acknowledges support from U.S. National Science Foundation grant ATM-94134337 and helpful conversations with P. L. Marston.

References

1. W. J. Humphries, *Physics of the Air* (McGraw-Hill, New York, 1929).
2. H. C. van de Hulst, *Light Scattering by Small Particles* (Wiley, New York, 1957).
3. J. A. Lock and L. Yang, "Mie theory of the corona," Appl. Opt. **30,** 3408–3414 (1991).
4. K. Sassen, "Corona producing cirrus cloud properties derived from polarization lidar and photographic analyses," Appl. Opt. **30,** 3421–3428 (1991).
5. K. Sassen, G. G. Mace, and J. Hallett, "Corona-producing ice clouds: a case study of a cold midlatitude cirrus layer," Appl. Opt. **37,** 1477–1485 (1998).
6. E. Trankle and B. Mielke, "Simulation and analysis of pollen coronas," Appl. Opt. **33,** 4552–4562 (1994).
7. L. M. Miloshevich and A. J. Heymsfield, "A balloon-borne continuous cloud particle replicator for measuring vertical profiles of cloud microphysical properties: instrument design, performance, and collection efficiency analysis," J. Atmos. Oceanogr. Technol. **14,** 753–768 (1997).
8. H. C. van de Hulst, "A theory of the anti-coronae," J. Opt. Soc. Am. **37,** 16–22 (1947).
9. J. D. Spinhirne and T. Nakajima, "Glory of clouds in the near infrared," Appl. Opt. **33,** 4652–4662 (1994).
10. D. K. Lynch and P. Schwartz, "Origin of the anthelion," J. Opt. Soc. Am. **69,** 383–386 (1979).
11. R. Greenler, *Rainbows, Halos, and Glories* (Cambridge U. Press, Cambridge, 1980), p. 145.
12. M. Kerker, *The Scattering of Light and Other Electromagnetic Radiation* (Academic, New York, 1969), Chap. 7.5.1.
13. T. S. Fahlen and H. C. Bryant, "Direct observation of surface waves on water droplets," J. Opt. Soc. Am. **56,** 1635–1636 (1966).
14. D. S. Langley and P. L. Marston, "Glory in backscattering from air bubbles," Phys. Rev. Lett. **47,** 913–916 (1981).
15. W. P. Arnott and P. L. Marston, "Optical glory of small freely rising gas bubbles in water: observed and computed cross-polarized backscattering patterns," J. Opt. Soc. Am. A **5,** 498–506 (1988).
16. W. P. Arnott and P. L. Marston, "Unfolded optical glory of spheroids: backscattering of laser light from freely rising spheroidal air bubbles in water," Appl. Opt. **30,** 3429–3442 (1991).
17. W. P. Arnott and P. L. Marston, "Unfolding axial caustics of glory scattering with harmonic angular perturbations of toroidal wavefronts," J. Acoust. Soc. Am. **85,** 1427–1440 (1989).
18. A. Mannoni, C. Flesia, P. Bruscaglioni, and A. Ismaelli, "Multiple scattering from Chebyshev particles: Monte Carlo simulations for backscattering in lidar geometry," Appl. Opt. **35,** 7151–7164 (1996).
19. S. Asano and M. Sato, "Light scattering by randomly oriented spheroidal particles," Appl. Opt. **19,** 962–974 (1980).
20. P. V. Hobbs, *Ice Physics* (Oxford U. Press, Oxford, 1974).
21. W. C. Thuman and E. Robinson, "Studies of Alaskan ice-fog particles," J. Meteorol. **11,** 151–156 (1954).
22. C. Magono, S.-I. Fujita, and T. Taniguchi, "Unusual types of single ice crystals originating from frozen cloud droplets," J. Atmos. Sci. **36,** 2495–2501 (1979).
23. B. Gonda and T. Yamazaki, "Initial growth of snow crystals growing from frozen cloud droplets," J. Meteorol. Soc. Jpn. **62,** 190–192 (1984).
24. D. Diermendjian, *Electromagnetic Scattering on Spherical Polydispersions* (Elsevier, New York, 1969).